

Research Article

Dynamic Modeling and Response of a Rotating Cantilever Beam with a Concentrated Mass

Yang Yong-feng,¹ Wang Yan-lin,¹ Chen Hu,^{1,2} and Wu Min-juan³

¹Institute of Vibration Engineering, Northwestern Polytechnical University, Xi'an 710072, China

²AECC Commercial Aircraft Engine CO., LTD, Shanghai 200241, China

³No. 771 Institute of Aerospace Times Electronics Corporation, Xi'an 710065, China

Correspondence should be addressed to Yang Yong-feng; yyf@nwpu.edu.cn

Received 12 July 2016; Revised 28 September 2016; Accepted 11 October 2016

Academic Editor: Toshiaki Natsuki

Copyright © 2016 Yang Yong-feng et al. This is an open access article distributed under the Creative Commons Attribution License, which permits unrestricted use, distribution, and reproduction in any medium, provided the original work is properly cited.

The rigid-flexible coupling system with a hub and concentrated mass is studied in this paper. Considering the second-order coupling of axial displacement which is caused by transverse deformation of the beam, the dynamic equations of the system are established using the second Lagrange equation and the assumed mode method. The simulation results show that the concentrated mass mainly suppresses the vibration and exhibits damping characteristics. When the nondimensional mass position parameter $\beta > 0.67$, the first natural frequency is reduced as the concentrated mass increases. When $\beta < 0.67$, the first natural frequency is increased as the concentrated mass increases. We also find the maximum first natural frequency nondimensional position for the concentrated mass.

1. Introduction

A classical motion mechanism in technical field of engineering and mechanical structures, such as space crafts, the robots, wind turbine blades, aircraft rotary wings, and the engine valves, is always reduced to a typical rotating cantilever beam. In order to design and control the dynamic behavior of those structures, it is necessary to estimate the modal characteristics and dynamical response. For the purpose of studying the basic characteristics, the model is simplified to a rigid-flexible coupling dynamical system consisting of both the flexible bodies and the rigid bodies. Southwell and Gough [1] derive the famous Southwell equation by using the Rayleigh energy theory to research the natural frequency of rotating beam. Then, to investigate further, some researchers combine Southwell equation with Ritz method [2, 3] to get a better simulation.

With the development of the dynamic stiffening and one-order coupling model, the study of vibration characteristics of the flexible cantilever beam has also entered a new stage [4–6]. Many researchers have studied the vibration control of the flexible cantilever beam [7–10]. For example, Ding et al. [11, 12] investigate the convergence of the Galerkin

method for the dynamic response of an elastic beam resting on a nonlinear foundation with viscous damping subject to a moving concentrated load. Zhang et al. [13] present experimental verifications of vibration suppression for a cantilever beam bond with a piezoelectric actuator by an adaptive controller. Li et al. [14] discuss the effects of the mass and position of the balance weight added in blades on the natural frequencies and mode shapes of the blades. By using the dynamic stiffness matrix method, Banerjee [15] studies the free vibration of axially loaded composite Timoshenko beams and applies his method to composite wings and helicopter blades. For the typical helicopter and wind turbine blades, Kambampati and Ganguli [16] assume the mass and stiffness distributions of the tapered rotating beam to be polynomial functions of span and find nonrotating beams that are isospectral to a given tapered rotating beam. Lee et al. [17, 18] give an exact power-series solution for free vibration of a rotating inclined Timoshenko beam. It is shown that both the extensional deformation and the Coriolis force will have significant influence on the natural frequencies of the rotating beam when the dimensionless rotating extension parameter is large. Even when the system parameters are changing, the vibration may show significant difference. In this paper, the

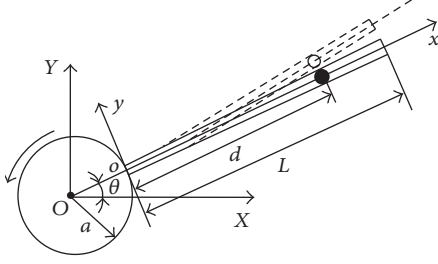


FIGURE 1: Rigid-flexible beam coupling system with concentrated mass.

rigid-flexible coupling system with a hub and concentrated mass is studied. Considering the second-order coupling of axial displacement which is caused by transverse deformation of the beam, the second Lagrange equation and assumed mode method are used to establish the dynamic equations. The influences of system parameters are analyzed.

2. The Dynamic Equations of Rigid-Flexible Coupling System

2.1. Dynamics Mode. In Figure 1, the rigid-flexible coupling system, which moves in the horizontal plane, is composed of the hub, flexible beam, and concentrated mass. The hub can rotate around the point O . The point o connects the hub and flexible beam. There is a concentrated mass on the beam. The extra excitation of the hub is τ . A fixed coordinate system O - XY is established at O , and a rotating coordinate system o - xy is established at the point o . The reverse extension line of x -axis passes O . This system can be divided into two parts: the hub and the flexible beam with the concentrated mass. All the parameters are presented in the Notations.

2.2. The Dynamic Equations of the System. According to the model of rigid-flexible coupling system, the kinetic energy of the whole system is

$$T = \frac{1}{2} \int_0^L \rho A \dot{\vec{r}} \cdot \dot{\vec{r}} dx + \frac{1}{2} I_h \dot{\theta}^2 + \frac{1}{2} m \dot{r}_d^2. \quad (1)$$

The potential energy is elastic deformation energy because the system is moving in the horizontal plane. That is,

$$V = \frac{1}{2} EI \int_0^L \left(\frac{\partial^2 v}{\partial x^2} \right)^2 dx + \frac{1}{2} EA \int_0^L \left(\frac{\partial^2 u}{\partial x^2} \right)^2 dx. \quad (2)$$

The coordinate transformation equation is

$$\begin{aligned} \dot{\vec{r}} &= \vec{V}_r + \vec{\phi} \times \vec{r} \\ &= (\dot{u} + \dot{u}_f - v\dot{\theta}) \vec{i}' + (\dot{v} + (x + u + u_f)\dot{\theta}) \vec{j}'. \end{aligned} \quad (3)$$

When using the assumed mode method, $v(x, t)$ can be expressed as $v(x, t) = \sum_{i=1}^n \phi_i(x) B_i(t)$, where $\phi_i(x)$ is the i th order modal shape functions of the transverse vibration

of a flexible beam; $B_i(t)$ is the i th order modal generalized coordinates; n is the modal order. $u_f(x, t)$ can be expressed as $u_f(x, t) = -(1/2) \int_0^x \sum_{i=1}^n \sum_{j=1}^n \phi_i'(\sigma) \phi_j'(\sigma) B_i B_j d\sigma$. Substituting (3) into (1) and (2), we can get

$$\begin{aligned} T &= \frac{1}{2} \rho A \dot{\theta}^2 \int_0^L \left((a + x + u_f)^2 + v^2 \right) dx \\ &+ \frac{1}{2} \rho A \int_0^L (\dot{v}^2 + \dot{u}_f^2) dx \\ &+ \rho A \dot{\theta}^2 \int_0^L (-v \dot{u}_f + \dot{v}(a + x + u_f)) dx + \frac{1}{2} I_h \dot{\theta}^2 \\ &+ \frac{1}{2} m \dot{r}_d^2, \end{aligned} \quad (4)$$

V

$$\begin{aligned} &= \frac{1}{2} \int_v E \varepsilon_{xx}^2 dv \\ &+ \rho A g \int_0^L \left((a + d + u_d + u_{fd}) \sin \theta + v \cos \theta \right) dx. \end{aligned}$$

Expand the expressions T and V

$$\begin{aligned} T &= \frac{1}{2} \rho A \dot{\theta}^2 \int_0^L \left((a + x + u_f)^2 + v^2 \right) dx + \frac{1}{2} \\ &\cdot m \left(\dot{\theta}^2 \left((a + d + u_{fd})^2 + v_d^2 \right) \right. \\ &+ \rho A \dot{\theta} \int_0^L (-v \dot{u}_f + \dot{v}(a + x + u_f)) dx + \frac{1}{2} \\ &\cdot \rho A \int_0^L (\dot{v}^2 + \dot{u}_f^2) dx + 2\dot{\theta} (-v_d \dot{u}_{fd} \\ &+ \dot{v}(a + d + u_{fd})) + \dot{v}_d^2 + \dot{u}_{fd}^2 \Big) = \frac{1}{2} \rho A \int_0^L \left(u^2 \right. \\ &+ u_f^2 + 2uu_f + v^2 \dot{\theta}^2 - 2iv\dot{\theta} - 2i\dot{u}_f v\dot{\theta} + x^2 \dot{\theta}^2 \\ &+ u^2 \dot{\theta}^2 \Big) dx + \frac{1}{2} \rho A \int_0^L \left(2u_f u \dot{\theta}^2 + \dot{v}^2 + u_f^2 \dot{\theta}^2 \right. \\ &+ 2ux\dot{\theta}^2 + 2u_f x\dot{\theta}^2 + 2xv\dot{\theta} + 2u\dot{v}\dot{\theta} \Big) dx + \frac{1}{2} \\ &\cdot \rho A \int_0^L \left(2u_f v\dot{\theta} + a^2 \dot{\theta}^2 + 2ax\dot{\theta}^2 + 2au\dot{\theta}^2 + 2au_f \dot{\theta}^2 \right. \\ &+ 2av\dot{\theta} \Big) dx + \frac{1}{2} m \left(\dot{\theta}^2 \left((a + d + u_{fd})^2 \right) \right. \\ &+ 2\dot{\theta} (-v_d \dot{u}_{fd} + \dot{v}(a + d + u_{fd})) + \dot{u}_{fd}^2 + \dot{v}_d^2 \Big) + \frac{1}{2} \\ &\cdot m \left(-2\dot{\theta} v_d \dot{u}_{fd} + \dot{\theta}^2 d^2 + \dot{\theta}^2 u_d^2 + \dot{\theta}^2 u_{fd}^2 + 2du_d \dot{\theta}^2 \right. \end{aligned}$$

$$\begin{aligned}
& + 2\dot{u}_{fd}\dot{u}_d + v_d^2\dot{\theta}^2) + \frac{1}{2}m(-2\dot{\theta}v_d\dot{u}_d + 2du_{fd}\dot{\theta}^2 \\
& + 2u_{fd}u_d\dot{\theta}^2 + \dot{v}_d^2 + 2d\dot{v}_d\dot{\theta} + 2u_d\dot{v}_d\dot{\theta} + 2u_{fd}\dot{v}_d\dot{\theta})) , \\
V = & \frac{1}{2} \int_v E\varepsilon_{xx}^2 dv + \rho Ag \int_0^L ((a + d + u_d + u_{fd}) \sin \theta \\
& + v \cos \theta) dx = \frac{1}{2} EA \int_0^L \left(\frac{\partial u}{\partial x} \right)^2 dx + \frac{1}{2} \\
& \cdot EI \int_0^L \left(\frac{\partial^2 v}{\partial x^2} \right)^2 dx \\
& + \rho Ag \int_0^L ((a + d + u_d + u_{fd}) \sin \theta \\
& + v \cos \theta) dx. \tag{5}
\end{aligned}$$

The dynamic equation of the system is established by Hamilton least action principle

$$\int_{t_1}^{t_2} (\delta T - \delta V + \delta W_f) dt = 0, \tag{6}$$

where δ means the variation of T , V , or W . W is the work of external force.

The kinetic equation of hub is

$$J_0 \ddot{\theta} = \tau. \tag{7}$$

According to the knowledge of structure dynamics, we assume the first two model functions of this system are

$$\phi_1(x) = A_1 \sin(\beta_1 x) + A_2 \cos(\beta_1 x), \tag{8}$$

$$\begin{aligned}
\phi_2(x) = & B_1 \sin(\beta_2 x) + B_2 \cos(\beta_2 x) + B_3 \sin h(\beta_2 x) \\
& + B_4 \cos h(\beta_2 x), \tag{9}
\end{aligned}$$

where $\beta_1^2 = \rho\omega^2/E$, $\beta_2^4 = \rho A\omega^2/EI$; A_1, A_2, B_1, B_2, B_3 , and B_4 are unknown parameters.

For the cantilever beam, the boundary conditions in axial direction are $\phi(0) = 0$, $\phi'(L) = 0$. We can get $A_2 = 0$, $\cos(\beta_1 x) = 0$.

The nature frequency is $\omega_i = ((2i-1)/2)(\pi/L)\sqrt{E/\rho}$, $i = 1, 2, \dots$, or $\omega_i = (1/2)(\pi/L)\sqrt{E/\rho}$, $i = 1, 3, 5, \dots$. The model functions are $\phi_1^i(x) = A_1 \sin(((2i-1)/2)(\pi/L)x)$, $i = 1, 2, \dots$

The boundary conditions in transverse direction are $\phi(0) = 0$, $\phi'(0) = 0$, $\phi'''(L) = 0$, $\phi''(L) = 0$. Here, 0 and L mean fix side and free side of the beam. Substituting those conditions into (9) yields $B_1 = -B_3$, $B_2 = -B_4$, and

$$\begin{aligned}
& B_1 (\cos(\beta_2 L) + \cos h(\beta_2 L)) \\
& + B_2 (\sin(\beta_2 L) + \sin h(\beta_2 L)) = 0, \\
& -B_1 (\sin(\beta_2 L) - \sin h(\beta_2 L)) \\
& + B_2 (\cos(\beta_2 L) - \cos h(\beta_2 L)) = 0. \tag{10}
\end{aligned}$$

The condition of nonzero solution for B_1 and B_2 is

$$\begin{vmatrix} \cos(\beta_2 L) + \cos h(\beta_2 L) & \sin(\beta_2 L) + \sin h(\beta_2 L) \\ -\sin(\beta_2 L) + \sin h(\beta_2 L) & -\cos(\beta_2 L) + \cos h(\beta_2 L) \end{vmatrix} = 0. \tag{11}$$

The solution for this equation is $\beta_2^1 L = 1.875$, $\beta_2^2 L = 4.694$, $\beta_2^3 L = 7.855$ when $i = 1, 2, 3$. When $i \geq 3$, $\beta_2^i L \approx ((2i-1)/2)\pi$. The nature frequencies are $\omega_i = (\beta_2^i L)\sqrt{EI/\rho AL^4}$, $i = 1, 2, \dots$. The model function is

$$\begin{aligned}
\phi_2^i(x) = & \cos(\beta_2^i x) - \cos h(\beta_2^i x) \\
& + \xi_i (\sin(\beta_2^i x) - \sin h(\beta_2^i x)), \tag{12} \\
& i = 1, 2, \dots,
\end{aligned}$$

where $\xi_i = (\cos(\beta_2^i x) + \cos h(\beta_2^i x))/(\sin(\beta_2^i x) + \sin h(\beta_2^i x))$, $i = 1, 2, \dots$

The orthogonal condition of the transverse modal function of the flexible beam is

$$\int_0^L \rho A \phi_m(x) \phi_n(x) dx = \begin{cases} 0 & m \neq n \\ 1 & m = n. \end{cases} \tag{13}$$

The dynamic equations can be written by the functions B_1 , B_2 , and θ as

$$\begin{aligned}
& \int_0^L (\rho A \phi_1^T \phi_1 \ddot{B}_1 - 2\rho A \phi_1^T \phi_2 \dot{B}_2 \dot{\theta} - \rho A \phi_1^T \phi_2 B_2 \ddot{\theta} \\
& - \rho A (a+x) \phi_1 \dot{\theta}^2 - \rho A \phi_1^T \phi_1 B_1 \dot{\theta}^2) dx \\
& - m(a+d) \phi_1(d) \dot{\theta}^2 + m(\phi_1^T(d) \phi_1(d) \ddot{B}_1 \\
& - 2\phi_1^T(d) \phi_2(d) \dot{B}_2 \dot{\theta} - \phi_1^T(d) \phi_2(d) B_2 \ddot{\theta}) \\
& + \int_0^L (EA \phi_1'^T \phi_1 B_1) dx - m \phi_1^T(d) \phi_1(d) B_1 \dot{\theta}^2 \\
& = 0, \\
& \int_0^L (\rho A \phi_2^T \phi_2 \ddot{B}_2 + 2\rho A \phi_1^T \phi_2 \dot{B}_1 \dot{\theta} - \rho A (a+x) \phi_2 \ddot{\theta} \\
& - \rho AB_1^T \phi_1^T \phi_2 \ddot{\theta} - \rho A \dot{\theta}^2 \phi_2^T \phi_2 B_2) dx - m((a \\
& + d) \phi_2(d) \ddot{\theta} - B_1^T \phi_1^T(d) \phi_2(d) \dot{\theta} - \dot{\theta}^2 \phi_2^T(d) \phi_2(d) \\
& \cdot B_2 + (a+d) H(d) B_2 \dot{\theta}^2) + \int_0^L (EI \phi_2''^T \phi_2'' B_2 + (a \\
& + x) HB_2 \dot{\theta}^2) dx + m(\phi_2^T(d) \phi_2(d) \ddot{B}_2 \\
& + 2\phi_1^T(d) \phi_2(d) \dot{B}_1 \dot{\theta}) = 0,
\end{aligned}$$

$$\begin{aligned}
& \int_0^L \rho A \left(\ddot{\theta} \left((a+x)^2 + B_2^T \phi_2^T \phi_2 B_2 + B_1^T \phi_1^T \phi_1 B_1 \right. \right. \\
& \quad \left. \left. + 2(a+x) \phi_1 B_1 - B_2^T (a+x) H B_2 \right) \right) dx \\
& \quad + B_1^T \phi_1^T (d) \phi_1 (d) B_1 + 2(a+d) \phi_1 (d) B_1 - (a+d) \\
& \quad \cdot B_2^T H (d) B_2 + (a+d) \phi_2 (d) \ddot{B}_2 + \int_0^L \rho A \left((a+x) \right. \\
& \quad \cdot \phi_2 \ddot{B}_2 + B_1^T \phi_1^T \phi_2 \ddot{B}_2 - B_2^T \phi_2^T \phi_1 \ddot{B}_1 - B_2^T (a+x) H B_2 \\
& \quad \left. + 2\dot{\theta} \left((a+x) \phi_1 \dot{B}_1 \right) \right) dx + B_1^T \phi_1^T (d) \phi_2 (d) \ddot{B}_2 \\
& \quad - B_2^T \phi_2^T (d) \phi_1 (d) \ddot{B}_1 + 2\dot{\theta} \left((a+d) \phi_1 (d) \dot{B}_1 \right. \\
& \quad \left. + B_1^T \phi_1^T (d) \phi_1 (d) \dot{B}_1 \right. \\
& \quad \left. + \int_0^L \rho A \left(2\dot{\theta} \left(B_1^T \phi_1^T \phi_1 \dot{B}_1 + B_2^T \phi_2^T \phi_2 \dot{B}_2 \right) \right) dx \right. \\
& \quad \left. + m \left(\dot{\theta} \left((a+d)^2 + B_2^T \phi_2^T (d) \phi_2 (d) B_2 \right. \right. \right. \\
& \quad \left. \left. + B_2^T \phi_2^T (d) \phi_2 (d) \dot{B}_2 - (a+d) B_2^T H (d) \dot{B}_2 \right) \right) \Big) \\
& = \tau,
\end{aligned} \tag{14}$$

where $H = \int_0^x (\partial \phi_2 / \partial \xi)^T (\partial \phi_2 / \partial \xi) d\xi$.

From (14), the ordinary differential equations can be rewritten into matrix form as

$$\begin{aligned}
& \begin{bmatrix} M_{\theta\theta} & \mathbf{M}_{\theta 1} & \mathbf{M}_{\theta 2} \\ \mathbf{M}_{1\theta} & \mathbf{M}_{11} & \mathbf{0} \\ \mathbf{M}_{2\theta} & \mathbf{0} & \mathbf{M}_{22} \end{bmatrix} \begin{bmatrix} \ddot{\theta} \\ \ddot{\mathbf{B}}_1 \\ \ddot{\mathbf{B}}_2 \end{bmatrix} + 2\dot{\theta} \begin{bmatrix} \mathbf{0} & \mathbf{0} & \mathbf{0} \\ \mathbf{0} & \mathbf{0} & \mathbf{G}_{12} \\ \mathbf{0} & \mathbf{G}_{21} & \mathbf{0} \end{bmatrix} \begin{bmatrix} \dot{\theta} \\ \dot{\mathbf{B}}_1 \\ \dot{\mathbf{B}}_2 \end{bmatrix} \\
& + \begin{bmatrix} \mathbf{0} & \mathbf{0} & \mathbf{0} \\ \mathbf{0} & \mathbf{k}_{11} & \mathbf{0} \\ \mathbf{0} & \mathbf{0} & \mathbf{k}_{22} \end{bmatrix} \begin{bmatrix} \theta \\ \mathbf{B}_1 \\ \mathbf{B}_2 \end{bmatrix} = \begin{bmatrix} \mathbf{Q}_\theta \\ \mathbf{Q}_1 \\ \mathbf{0} \end{bmatrix},
\end{aligned} \tag{15}$$

where

$$\begin{aligned}
M_{\theta\theta} &= \int_0^L \rho A (x+a)^2 dx + m(d+a)^2 + \mathbf{B}_1^T \mathbf{M}_{11} \mathbf{B}_1 \\
& \quad + \mathbf{B}_2^T \mathbf{M}_{22} \mathbf{B}_2 + 2(\mathbf{U}_{11} + a\mathbf{U}_{10}) \mathbf{B}_1 - \mathbf{B}_2^T (\mathbf{D}_1 + a\mathbf{D}_0) \\
& \quad \cdot \mathbf{B}_2, \\
\mathbf{M}_{1\theta} &= \mathbf{M}_{\theta 1}^T = -\mathbf{R} \mathbf{B}_2, \\
\mathbf{M}_{\theta 2} &= \mathbf{M}_{2\theta}^T = \mathbf{U}_{12} + \mathbf{B}_1^T \mathbf{R} + a\mathbf{U}_{20}, \\
\mathbf{G}_{12} &= -\mathbf{G}_{21}^T = -\mathbf{R},
\end{aligned}$$

$$\mathbf{M}_{11} = \int_0^L \rho A \phi_1^T \phi_1 dx + m \phi_1^T (d) \phi_1 (d),$$

$$\mathbf{M}_{22} = \int_0^L \rho A \phi_2^T \phi_2 dx + m \phi_2^T (d) \phi_2 (d),$$

$$\mathbf{K}_{11} = \mathbf{K}_1 - \dot{\theta}^2 \mathbf{M}_{11},$$

$$\mathbf{Q}_1 = \dot{\theta}^2 (\mathbf{U}_{11} + a\mathbf{U}_{10})^T,$$

$$\mathbf{K}_1 = \int_0^L EA \phi_1'^T \phi_1' dx,$$

$$\mathbf{K}_2 = \int_0^L EI \phi_2''^T \phi_2'' dx,$$

$$\mathbf{K}_{22} = \mathbf{K}_2 - \dot{\theta}^2 \mathbf{M}_{22} + \dot{\theta}^2 (\mathbf{D}_1 + a\mathbf{D}_0),$$

$$\mathbf{U}_{1j} = \int_0^L \rho A x \phi_j (x) dx + m d \phi_j (d), \quad j = 1, 2,$$

$$\begin{aligned}
\mathbf{Q}_\theta &= -2\dot{\theta} (\mathbf{B}_1^T \mathbf{M}_1 \dot{\mathbf{B}}_1 + \mathbf{B}_2^T \mathbf{M}_2 \dot{\mathbf{B}}_2 + (\mathbf{U}_{11} + a\mathbf{U}_{10}) \dot{\mathbf{B}}_1 \\
& \quad - \mathbf{B}_2^T (\mathbf{D}_1 + a\mathbf{D}_0) \dot{\mathbf{B}}_2),
\end{aligned}$$

$$\mathbf{D}_0 = \int_0^L \rho A \mathbf{Z} (x) dx + m \mathbf{Z} (d),$$

$$\mathbf{D}_1 = \int_0^L \rho A x \mathbf{Z} (x) dx + m d \mathbf{Z} (d),$$

$$\mathbf{U}_{10} = \int_0^L \rho A \phi_1 (x) dx,$$

$$\mathbf{R} = \int_0^L \rho A \phi_1^T \phi_2 dx + m \phi_1^T (d) \phi_2 (d),$$

$$\mathbf{U}_{20} = \int_0^L \rho A \phi_2 (x) dx + m \phi_2 (d),$$

$$\mathbf{Z} (d) = \int_0^d \phi_2'^T (\sigma) \phi_2' (\sigma) d\sigma.$$

(16)

3. Dynamical Simulations

3.1. First Natural Frequency Analysis. For the study of [6], the coupling effect between stretching and bending motions can be ignored for slender beams and the natural frequencies of stretching motion are far greater than those of bending motion. Therefore, the bending vibration equation of the beam can be expressed as

$$M_{22} \ddot{B}_2 + \left(K_2 - \dot{\theta}^2 M_{22} + \dot{\theta}^2 (D_1 + aD_0) \right) B_2 = 0, \tag{17}$$

where $\overline{M}_{22} = \int_0^1 \phi_2^T \phi_2 d\xi + \alpha \phi_2^T (\beta) \phi_2 (\beta)$, $\overline{K}_2 = \int_0^1 \phi_2''^T \phi_2'' d\xi$, $\overline{Z} (\xi) = \int_0^\xi (\partial \phi_2 / \partial \eta)^T (\partial \phi_2 / \partial \eta) d\eta$, $\overline{U}_{12}^T = (\int_0^1 (\delta + \xi) \phi_2 d\xi + \alpha \phi_2 (\beta))^T$, $\overline{D}_1 = \int_0^1 (\delta + \xi) \overline{Z} (\xi) d\xi + \alpha \cdot (\delta + \beta) \int_0^\beta \phi_2'^T (\xi) \phi_2' (\xi) d\xi$.

The nondimensional form of (17) can be obtained:

$$\overline{M}_{22}\ddot{k}_2 + (\overline{K}_2 - \gamma^2\overline{M}_{22} + \gamma^2\overline{D}_1)k_2 = -\chi\overline{U}_{12}^T, \quad (18)$$

where the nondimensional parameters are

$$\begin{aligned} \zeta &= \frac{t}{T}, \\ \xi &= \frac{x}{L}, \\ k_2 &= \frac{B_2}{L}, \\ \delta &= \frac{a}{L}, \\ \gamma &= T\dot{\theta}, \\ \alpha &= \frac{m}{\rho AL}, \\ \beta &= \frac{d}{L}, \\ \chi &= T^2\ddot{\theta}, \\ T &= \left(\frac{\rho AL^4}{EI} \right)^{1/2}. \end{aligned} \quad (19)$$

The natural frequency of rotating cantilever beam with a concentrated mass can be studied by solving the eigenvalue problem for (18). The harmonic function of the nondimensional time ζ can be expressed as

$$k_2 = e^{jf\zeta}\Theta, \quad (20)$$

where j is an imaginary number; f is nondimensional frequency; Θ is a constant column matrix. Substituting (18) into (20) yields

$$\omega^2 M\Theta = K^C\Theta, \quad (21)$$

where M and K^C are square matrices, which are, respectively, defined as $M = \overline{M}_{22}$, $K^C = -\gamma^2\overline{M}_{22} + \gamma^2\overline{D}_1$.

The simulation parameters are as follows: length of beam $L = 8$ m, radius of the hub $a = 8$ m, cross section area of the beam $A = 7.2968 \times 10^{-5}$ m², moment of inertia of cross section $I = 8.2189 \times 10^{-9}$ m⁴, density $\rho = 2.7667 \times 10^3$ kg/m³, and elastic modulus $E = 6.8952 \times 10^{10}$ N/m².

Figure 2 shows the effect of the concentrated mass on the first natural frequency. The nondimensional position for the numerical results is $\beta = 1$ (at the free end of cantilever beam). The natural frequency curves are lowered when the concentrated mass increases. However, the lowering effect is attenuated as the concentrated mass ratio increases.

Figure 3 shows the effect of the location of a concentrated mass on the first natural frequency. With the concentrated mass moving from the fixed end to the free end, the first natural frequencies first increase and then decrease. The variation increases as the concentrated mass increases. The

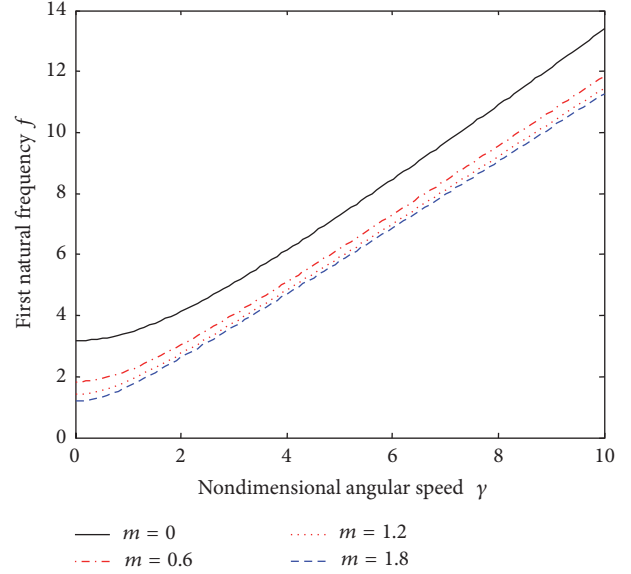


FIGURE 2: Effect of the concentrated mass on the first natural frequency.

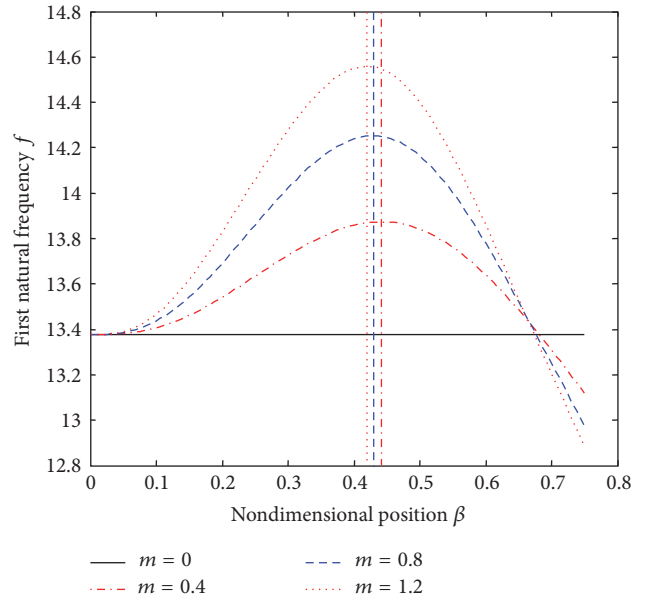


FIGURE 3: Effect of the concentrated mass location on the first natural frequency.

crossover point of these curves is around $\beta = 0.67$. When $m = 0.4$ kg, the maximum value position of first natural frequency is $\beta = 0.442$. When $m = 0.8$ kg, the maximum value position is $\beta = 0.429$. When $m = 1.2$ kg, the maximum value position is $\beta = 0.42$. The maximum values position decreases with the increasing of mass.

3.2. The Effect of the Concentrated Mass on the Flexible Beam. The angular velocity of large range motion is supposed as an

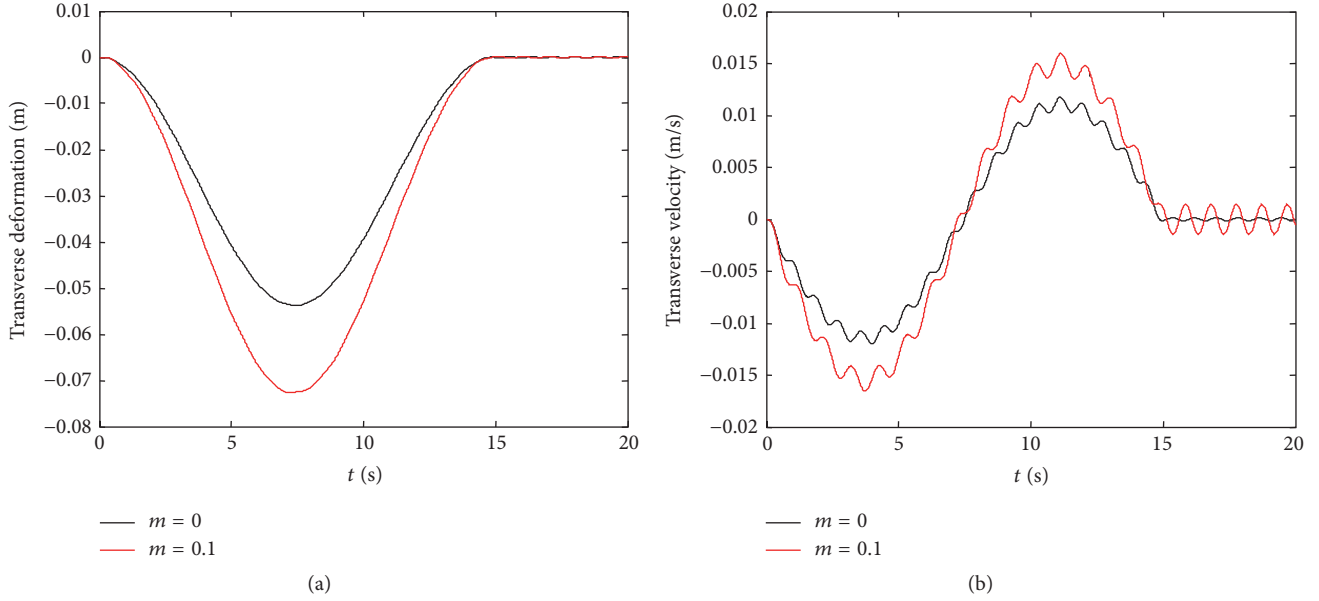


FIGURE 4: Effect of the concentrated mass on the response when flexible beam is subjected to acceleration process, (a) deformation and (b) velocity.

acceleration process

$$\dot{\theta} = \begin{cases} \frac{\omega_0}{T}t - \frac{\omega_0}{2\pi} \sin\left(\frac{2\pi}{T}t\right), & 0 \leq t \leq T \\ \omega_0, & t > T. \end{cases} \quad (22)$$

When the time is $T = 15$ s, the angular speed of the flexible beam became rotating with a constant speed $\omega_0 = 10$ rad/s. The simulation parameters are as follows: length of beam $L = 8$ m, radius of the hub $a = 0$, cross section area of the beam $A = 7.2968 \times 10^{-5}$ m², moment of inertia of cross section $I = 8.2189 \times 10^{-9}$ m⁴, density $\rho = 2.7667 \times 10^3$ kg/m³, and elastic modulus $E = 6.8952 \times 10^{10}$ N/m². When the concentrated mass position parameter $\beta = 1$, the effects of concentrated mass on the dynamical response are shown in Figure 4. The free end vibration of flexible beam has been increased by the concentrated mass. The velocity and deformation with concentrated mass are bigger than those without concentrated mass. The variable of response is aggravated by concentrated mass at the free end.

For another situation, supposing that there is a sine function couple on the hub. The couple with time variable can be written as

$$\tau(t) = \begin{cases} \tau_0 \sin\left(\frac{2\pi}{T}t\right), & 0 \leq t \leq T \\ 0, & t > T, \end{cases} \quad (23)$$

where $\tau_0 = 1$ N·m, $T = 10$ s. The parameter β is 1. After 10 s, the couple is 0. Figure 5 shows the response of angular displacement and transverse deformation. From 0 to 10 s, the angular displacement of the free end of the beam has been depressed by the concentrated mass increasing. There exist periodic vibrations after the couple of forces change to 0. The transverse deformation has been slightly increased by concentrated mass. However, the concentrated mass stables

the vibration of the free end of the beam. All these show that the concentrated mass mainly suppresses the vibration and exhibits damping characteristics.

4. Conclusion

By establishing the dynamics model of rigid-flexible coupling system, the dynamic equation of the flexible beam with concentrated mass is derived in this paper. The main conclusions were as follows:

- (1) When the nondimensional mass position parameter $\beta > 0.67$, the first natural frequency is reduced when the concentrated mass increases. When $\beta < 0.67$, the first natural frequency is increased when the concentrated mass increases. By considering the high order coupling, the critical value 0.67 is a better prediction and a simulation value for this system. Further experiment is needed to get the true value.
- (2) The maximum first natural frequency position is near 0.42 (nondimensional mass position parameter) when the concentrated mass increases, comparing with the result 0.4 in [6] which does not consider the high order coupling.
- (3) The concentrated mass mainly suppresses the vibration and exhibits damping characteristics.

Notations

Summary of the General Notation Used in Figure 1

- a : Radius of the hub
 J_{oh} : Moment of inertia of the central rigid body around O

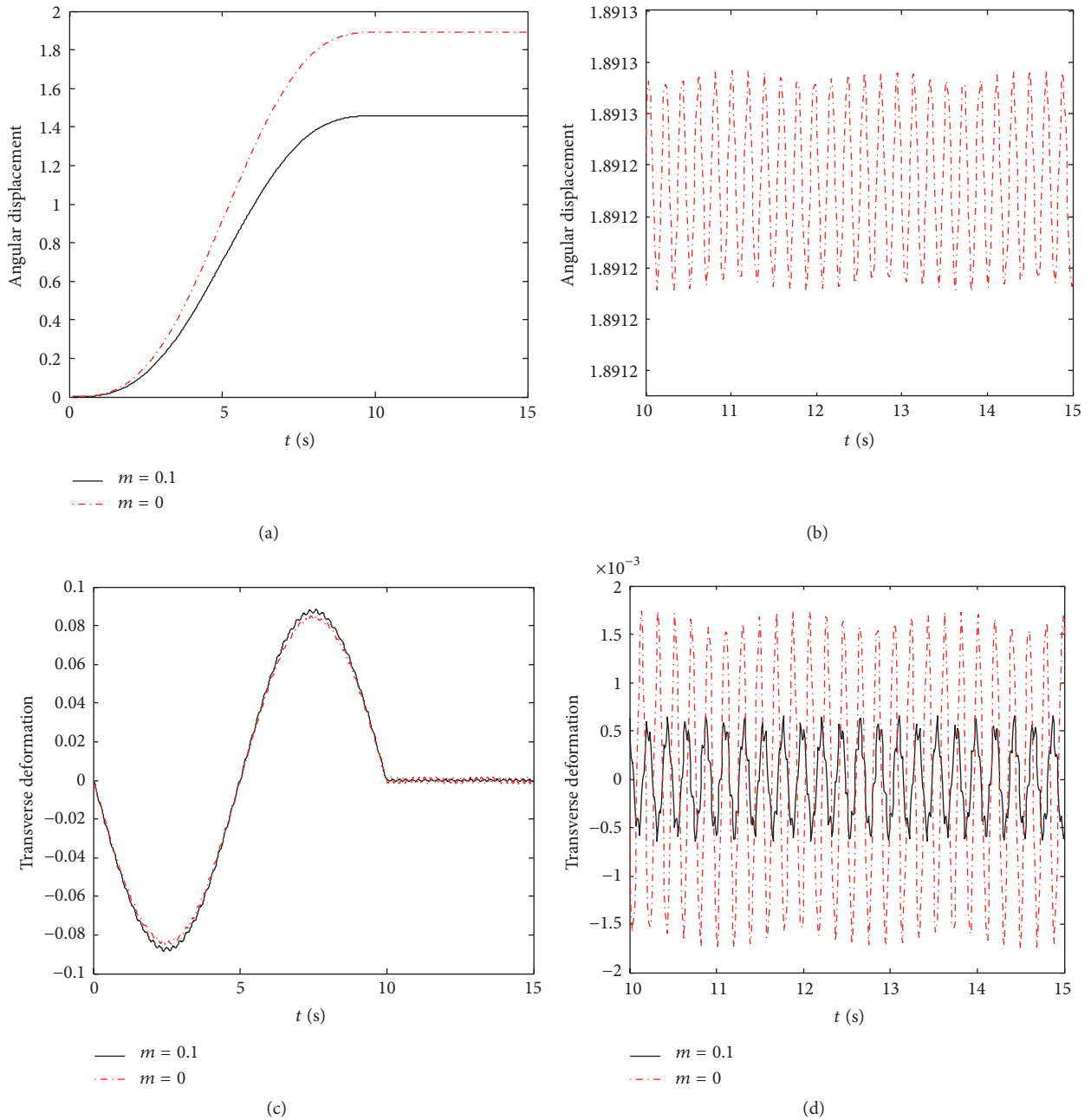


FIGURE 5: Effect of the concentrated mass on the angular displacement and transverse deformation when flexible beam is subjected to a sine function couple: (a) angular displacement, (b) local diagram of angular displacement, (c) transverse deformation, and (d) local diagram of transverse deformation.

- L : Length of the flexible beam
- ρAL : Mass of the flexible beam
- EA : Tension and compression stiffness of the flexible beam
- EI : Bending stiffness of the flexible beam
- J_{ob} : Moment of inertia of the flexible beam around O
- m : Quality of concentrated mass
- r_d : Concentrated mass position on the beam
- d : Distance between the concentrated mass and o
- θ : Angle between the beam and the x -axis.

Competing Interests

The authors declare that there is no conflict of interests regarding the publication of this paper.

Acknowledgments

This work was supported by the National Natural Science Foundation of China (Grant nos. 11272257 and 11672237) and NPU Aoxiang New Star.

References

- [1] R. Southwell and F. Gough, "The free transverse vibration of airscrew blades," British ARC Reports and Memoranda 766, 1921.
- [2] S. Putter and H. Manor, "Natural frequencies of radial rotating beams," *Journal of Sound and Vibration*, vol. 56, no. 2, pp. 175–185, 1978.
- [3] A. D. Wright, C. E. Smith, R. W. Thresher, and J. L. C. Wang, "Vibration modes of centrifugally stiffened beams," *Journal of Applied Mechanics*, vol. 49, no. 1, pp. 197–202, 1982.
- [4] H. H. Yoo and S. H. Shin, "Vibration analysis of rotating cantilever beams," *Journal of Sound and Vibration*, vol. 212, no. 5, pp. 807–828, 1998.
- [5] J. Cheng, H. Xu, and A. Yan, "Frequency analysis of a rotating cantilever beam using assumed mode method with coupling effect," *Mechanics Based Design of Structures and Machines*, vol. 34, no. 1, pp. 25–47, 2006.
- [6] H. H. Yoo, S. Seo, and K. Huh, "The effect of a concentrated mass on the modal characteristics of a rotating cantilever beam," *Proceedings of the Institution of Mechanical Engineers, Part C: Journal of Mechanical Engineering Science*, vol. 216, no. 2, pp. 151–163, 2002.
- [7] F. B. Sayyad and N. D. Gadhav, "Variable stiffness type magnetic vibration absorber to control the vibration of beam structure," *Journal of Vibration and Control*, vol. 20, no. 13, pp. 1960–1966, 2014.
- [8] M. S. Saad, H. Jamaluddin, and I. Z. M. Darus, "Active vibration control of a flexible beam using system identification and controller tuning by evolutionary algorithm," *Journal of Vibration and Control*, vol. 21, no. 10, pp. 2027–2042, 2013.
- [9] A. P. Parameswaran and K. V. Gangadharan, "Parametric modeling and FPGA based real time active vibration control of a piezoelectric laminate cantilever beam at resonance," *Journal of Vibration & Control*, vol. 21, no. 14, pp. 2881–2895, 2015.
- [10] M. A. Nojournian, R. Vatankhah, and H. Salarieh, "Vibration suppression of a strain gradient micro-scale beam via an adaptive lyapunov control strategy," *Journal of Dynamic Systems Measurement and Control*, vol. 138, no. 3, pp. 1472–1477, 2016.
- [11] H. Ding, L.-Q. Chen, and S.-P. Yang, "Convergence of Galerkin truncation for dynamic response of finite beams on nonlinear foundations under a moving load," *Journal of Sound and Vibration*, vol. 331, no. 10, pp. 2426–2442, 2012.
- [12] H. Ding and L.-Q. Chen, "Galerkin methods for natural frequencies of high-speed axially moving beams," *Journal of Sound and Vibration*, vol. 329, no. 17, pp. 3484–3494, 2010.
- [13] T. Zhang, H. G. Li, Z. Y. Zhong, and G. P. Cai, "Hysteresis model and adaptive vibration suppression for a smart beam with time delay," *Journal of Sound and Vibration*, vol. 358, pp. 35–47, 2015.
- [14] L. Li, Y. H. Li, Q. K. Liu, and B. K. Jiang, "Effect of balance weight on dynamic characteristics of a rotating wind turbine blade," *Journal of Engineering Mathematics*, vol. 97, no. 1, pp. 49–65, 2016.
- [15] J. R. Banerjee, "Free vibration of axially loaded composite Timoshenko beams using the dynamic stiffness matrix method," *Computers & Structures*, vol. 69, no. 2, pp. 197–208, 1998.
- [16] S. Kambampati and R. Ganguli, "Nonrotating beams isospectral to tapered rotating beams," *AIAA Journal*, vol. 54, no. 2, pp. 750–757, 2016.
- [17] S. Y. Lee and J. J. Sheu, "Free vibration of an extensible rotating inclined Timoshenko beam," *Journal of Sound and Vibration*, vol. 304, no. 3–5, pp. 606–624, 2007.
- [18] S.-Y. Lee, J.-J. Sheu, and S.-M. Lin, "In-plane vibrational analysis of rotating curved beam with elastically restrained root," *Journal of Sound and Vibration*, vol. 315, no. 4-5, pp. 1086–1102, 2008.



Hindawi

Submit your manuscripts at
<http://www.hindawi.com>

